Coral Reefs (2016) 35:681–693
DOI 10.1007/s00338-015-1383-y

REPORT

Spatial and seasonal reef calcification in corals and calcareous crusts in the central Red Sea

Anna Roik[1] · Cornelia Roder[1] · Till Röthig[1] · Christian R. Voolstra[1]

Received: 12 April 2015 / Accepted: 27 November 2015 / Published online: 14 December 2015
© The Author(s) 2015. This article is published with open access at Springerlink.com

Abstract The existence of coral reef ecosystems critically relies on the reef carbonate framework produced by scleractinian corals and calcareous crusts (i.e., crustose coralline algae). While the Red Sea harbors one of the longest connected reef systems in the world, detailed calcification data are only available from the northernmost part. To fill this knowledge gap, we measured in situ calcification rates of primary and secondary reef builders in the central Red Sea. We collected data on the major habitat-forming coral genera *Porites*, *Acropora*, and *Pocillopora* and also on calcareous crusts (CC) in a spatio-seasonal framework. The scope of the study comprised sheltered and exposed sites of three reefs along a cross-shelf gradient and over four seasons of the year. Calcification of all coral genera was consistent across the shelf and highest in spring. In addition, *Pocillopora* showed increased calcification at exposed reef sites. In contrast, CC calcification increased from nearshore, sheltered to offshore, exposed reef sites, but also varied over seasons. Comparing our data to other reef locations, calcification in the Red Sea was in the range of data collected from reefs in the Caribbean and Indo-Pacific; however, *Acropora* calcification estimates were at the lower end of worldwide rates. Our study shows that the increasing coral cover from nearshore to offshore environments aligned with CC calcification but not coral calcification, highlighting the potentially important role of CC in structuring reef cover and habitats. While coral calcification maxima have been typically observed during summer in many reef locations worldwide, calcification maxima during spring in the central Red Sea indicate that summer temperatures exceed the optima of reef calcifiers in this region. This study provides a foundation for comparative efforts and sets a baseline to quantify impact of future environmental change in the central Red Sea.

Keywords Coral reef · Calcification · Red Sea · Buoyant weight · Seasonality · Cross-shelf gradient

Introduction

Tropical coral reefs are of unique value with regard to ecosystem productivity as well as species diversity (Wilkinson 2008). Their ecological importance is intimately linked to the structural complexity of the habitat (Goreau 1963), which is essential for the existence of most reef organisms (Graham 2014). Biogenic reef calcification, which is limited to tropical shorelines of warm, clear, sunlit waters, and relatively stable physical conditions (Kleypas et al. 1999), is a key process contributing to reef habitat complexity. Scleractinian corals are the primary reef builders that deposit calcium carbonate ($CaCO_3$) to give rise to the three-dimensional reef framework. Secondary reef builders, composed predominantly of crustose coralline algae (Corallinales), form calcareous crusts (CC) and fortify the reef framework through cementation, counteracting its disintegration through erosion processes (Mallela and Perry 2007; Perry and Hepburn 2008).

Communicated by Biology Editor Dr. Simon Davy

Electronic supplementary material The online version of this article (doi:10.1007/s00338-015-1383-y) contains supplementary material, which is available to authorized users.

✉ Christian R. Voolstra
christian.voolstra@kaust.edu.sa

[1] Red Sea Research Center, King Abdullah University of Science and Technology (KAUST), Building 2, Level 2, Thuwal, Kingdom of Saudi Arabia

In scleractinian corals, calcification depends on the productivity of the intracellular dinoflagellate algal symbionts (commonly referred to as zooxanthellae) that supply energy to the coral host through photosynthesis (Muscatine 1990). In addition, calcification rates in corals can further increase through heterotrophic feeding on plankton and suspended matter in the water column (Houlbrèque and Ferrier-Pagès 2009). CC calcification (considering Corallinales), in comparison, is directly based on the algae's physiology and depends on factors that support photosynthesis (reviewed in Borowitzka and Larkum 1987) such as availability of light and inorganic nutrients (Chalker 1981; Chisholm 2000; Ferrier-Pagès et al. 2000).

Calcification rates are considered to be most sensitive to changes in temperature (Castillo et al. 2014), although the aragonite saturation state is also a determining factor (Gattuso et al. 1998; Martin and Gattuso 2009). High temperatures have been shown to positively impact coral growth, leading to calcification maxima during summer conditions (Crossland 1984; Hibino and van Woesik 2000; Kuffner et al. 2013) and to higher calcification at warmer, lower latitudes compared to cooler, higher latitudes (Lough and Barnes 2000; Carricart-Ganivet 2004). Yet, calcification rates can be fitted to a Gaussian distribution with a calcification maximum indicating the optimal temperature and calcification limits toward high- and low-temperature values (Marshall and Clode 2004). Indeed, reduced calcification has been shown to be associated with a rise in sea surface temperatures (SST), even when bleaching is not present (Cooper et al. 2008; Cantin et al. 2010; Carricart-Ganivet et al. 2012). Hence, coral growth and calcification rates are considered a diagnostic tool to provide insight into the performance and health status of corals (Edinger et al. 2000; Wooldridge 2014).

The majority of coral reefs thrive in stable physico-chemical environments with temperatures typically not exceeding 29 °C and salinities around 36 PSU (Kleypas et al. 1999), which is typically most favorable to coral growth. The Red Sea deviates from these environmental settings, with sea surface temperatures (SSTs) reaching 32 °C in the summer, temperature differences of up to 10 °C throughout the annual cycle (Davis et al. 2011), and a relatively high salinity of 40 PSU or higher (Abu-Ghararah 1997). Yet, the Red Sea features a high $CaCO_3$ saturation state (Steiner et al. 2014) and low sediment loads (Abu-Ghararah 1997), both of which can be considered beneficial for calcification. Indeed, pelagic $CaCO_3$ precipitation rates in the Red Sea were estimated to be higher than in the Gulf of Aden or the Indian Ocean (Steiner et al. 2014), but a comprehensive study collecting in situ reef calcification rates is missing.

To provide a baseline of reef calcification data for the reefs in the central Red Sea, we quantified in situ calcification rates as mass increments over time using the buoyant weight technique (Davies 1989) in a multispecies framework including primary and secondary reef builders and spanning different reef locations across the shelf and across four seasons. Further, using spatial calcification rates of different calcifiers, we investigated whether and how their calcification performance relates to their benthic abundance in reef sites. Moreover, we explored the relationship of temperature and seasonal calcification rates using in situ temperature records. By comparing the resulting annual average calcification rates from the central Red Sea with data from the Caribbean and the Indo-Pacific, we examined whether the unique environmental setting encountered in the Red Sea (warm, clear, sunlit, and highly carbonate saturated waters) potentially maintains higher reef calcification compared to other coral reef regions.

Materials and methods

Study sites and seasons

Data for this study were collected at the exposed (fore reef) and sheltered (back reef) sites of three reefs, comprising six sites along a cross-shelf gradient off the Saudi Arabian coast (Fig. 1): offshore exposed and sheltered (Shi'b Nazar reef, 22° 20.456N, 38° 51.127E); midshore exposed and sheltered (Al Fahal reef, 22° 15.100N, 38° 57.386E); and inshore exposed and sheltered (Inner Fsar reef, 22° 13.974N, 39° 01.760E). All study sites were located between 7.5 and 9 m depth. The study sites represented reefs of different environmental conditions, ranging from well-mixed habitats exposed to the open sea to turbid lagoonal inshore waters (Fig. 2a).

Four seasons were measured consecutively over 3-month intervals during one full year from mid-September 2012 to mid-September 2013 for corals and from mid-December 2012 to mid-December 2013 for CC. Seasons were defined as follows: spring from 15 March 2013 to 15 June 2013; summer from 15 June 2013 to 15 September 2013; fall from 15 September 2012 to 15 December 2012 (for coral assessment) or 15 September 2013 to 15 December 2013 (for CC assessment); and winter from 15 December 2012 to 15 March 2013.

Benthic reef composition

To characterize the study sites, benthic reef composition was surveyed between October and December 2013. We followed a modified rugosity transect methodology from Perry et al. (2012). While standard line-intercept methods may underestimate the coverage of cryptic benthic components (e.g., coralline algae), the rugosity transect provides better resolution in this regard (Goatley and

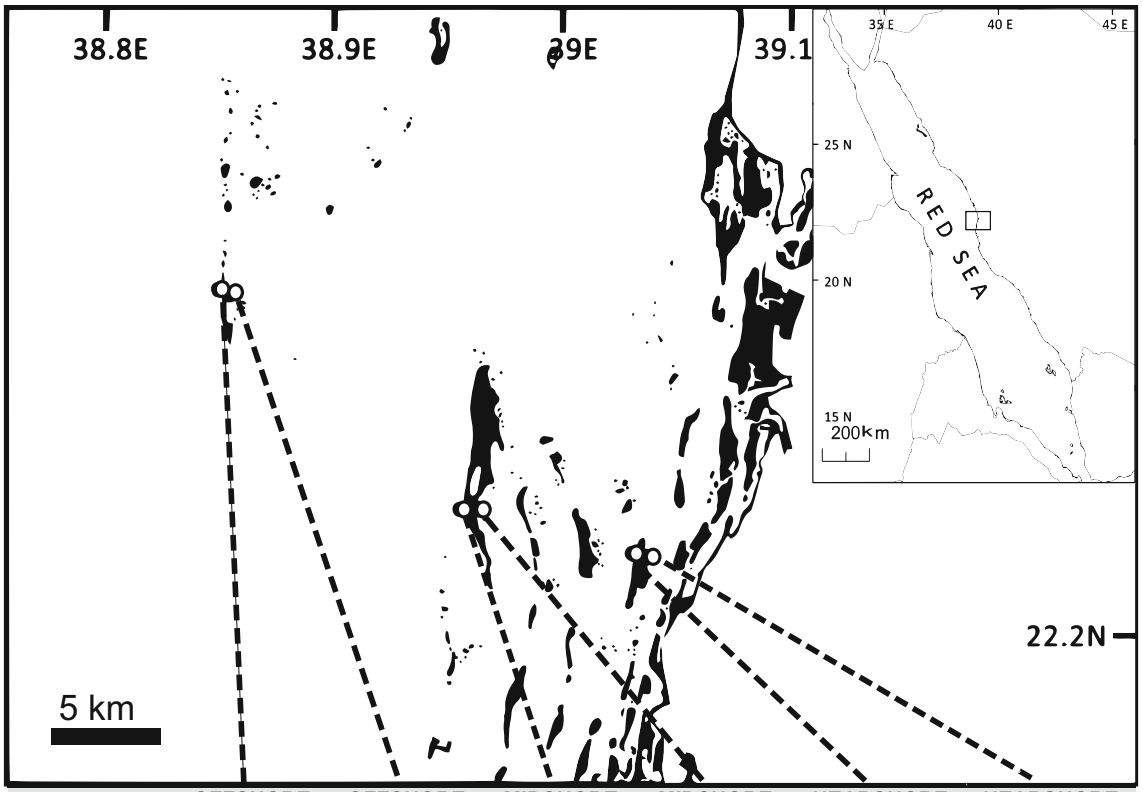

	OFFSHORE EXPOSED	OFFSHORE SHELTERED	MIDSHORE EXPOSED	MIDSHORE SHELTERED	NEARSHORE EXPOSED	NEARSHORE SHELTERED
coordinates	22°20.456 N 38°51.127 E	22°20.502 N 38°51.245 E	22°15.100 N 38°57.386 E	22°15.119 N 38°57.761 E	22°13.974 N 39°01.760 E	22°13.850 N 39°02.216 E
distance from shore	25 km	25 km	10 km	10 km	3 km	3 km
	replicates per season					
SPRING	POR (5) ACR (6) POC (6) CC (5)	POR (4) ACR (7) POC (6) CC (5)	POR (5) ACR (6) POC (5) CC (5)	POR (6) ACR (10) POC (7) CC (6)	POR (8) ACR (7) CC (3)	POR (8) ACR (6) CC (5)
SUMMER	POR (5) ACR (6) POC (6) CC (2)	POR (4) ACR (7) POC (6) CC (5)	POR (7) ACR (4) POC (4) CC (5)	POR (6) ACR (10) POC (6) CC (4)	POR (8) ACR (6) CC (4)	POR (7) ACR (5) CC (5)
FALL	POR (5) ACR (6) POC (5) CC (0)	POR (6) ACR (7) POC (5) CC (1)	POR (3) ACR (6) POC (5) CC (1)	POR (4) ACR (4) POC (2) CC (5)	POR (1) ACR (4) CC (5)	POR (6) ACR (4) CC (6)
WINTER	POR (5) ACR (5) POC (5) CC (6)	POR (6) ACR (4) POC (5) CC (5)	POR (5) ACR (4) POC (6) CC (6)	POR (4) ACR (5) POC (3) CC (6)	POR (7) ACR (4) CC (5)	POR (2) ACR (6) CC (6)

Fig. 1 Overview of spatio-seasonal study design. The reef map provides location of the six study sites along the cross-shelf gradient. The table includes the site coordinates, site distance from shore, and replicate numbers (*in brackets*) for each calcifier group in each reef site (POR, *Porites*; ACR, *Acropora*; POC, *Pocillopora*; CC, calcareous crusts, image credits: Maha Khalil)

Bellwood 2011) as it follows reef topography. Six replicate transects (10 m long, spaced 10 m apart) at depths of 7.5–9 m were sampled parallel to the reef front. We considered the following benthic categories: sand/silt; rubble; rock; recently dead coral; macro- and turf algae; sponges; soft coral; other non-calcifying benthic reef organisms; and CC. Further, we recorded subcategories for the major reef-building taxa *Porites* spp., *Acropora* spp., and *Pocillopora* spp. and categorized other corals according to major growth forms as other branching, other massive corals, encrusting, and plate/foliose corals. Data were prepared as means and standard deviations of six replicate transects per reef (ESM Table S1).

Temperature profiles

Temperature loggers (SBE 16plusV2 SEACAT, RS-232, Sea-Bird Electronics, Bellevue, WA, USA) were deployed

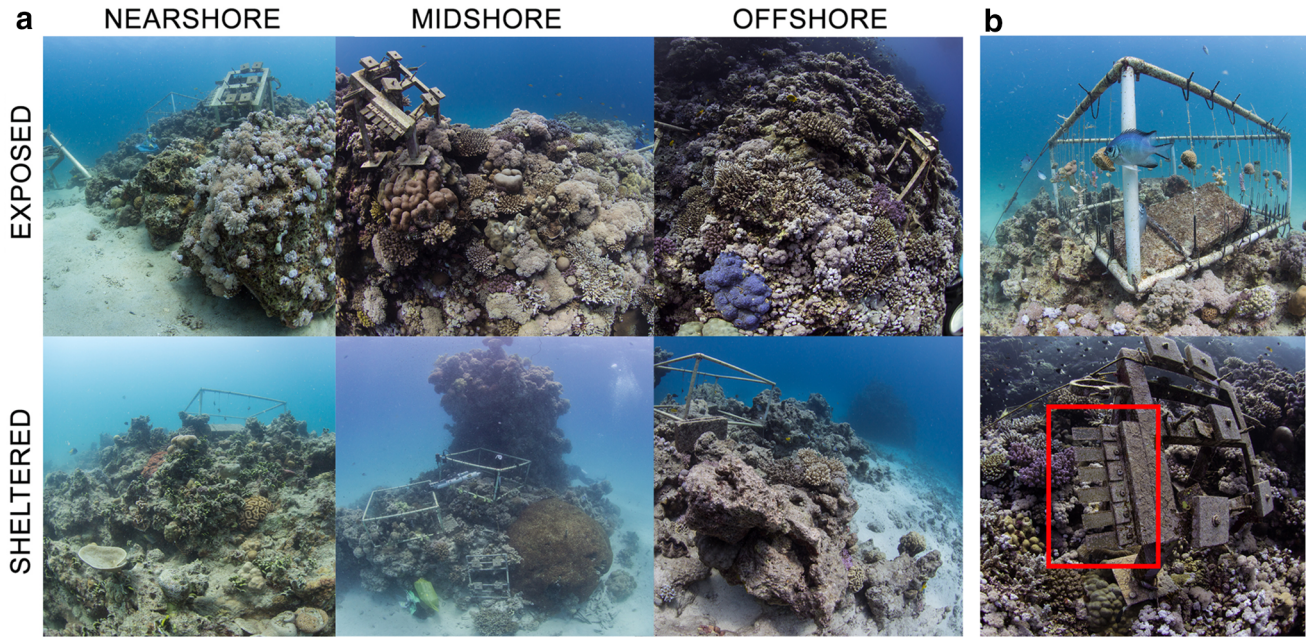

Fig. 2 Study sites and in situ setup of moored frames. **a** The study sites along the cross-shelf gradient, which represent reefs ranging from exposed fore-reef well-mixed habitats to turbid back-reef lagoonal waters. **b** Moored frames, deployed at a study site, demonstrate how coral fragments (*top*) and plastic microscope slides (*red box*, *bottom*) were attached. Photographs: Anna Roik

at the exposed study sites of each shelf section within the four seasons of the year in parallel with the assessment of coral calcification (see details above). For logistical reasons and due to battery life times of available loggers, sheltered sites were equipped with temperature loggers (TidbiT v2 temp, resolution 0.02 °C, accuracy 0.2 °C, Onset, Bourne, MA, USA) only during summer and winter seasons (summer deployment: 22 July 2013 to 11 September 2013; winter deployment: 25 November 2012 to 2 February 2013). For the time series plot, hourly logged data were smoothed through a weekly moving average filter. Additionally, the overall annual mean and standard deviation were determined. Moreover, we provide temperature averages, standard deviations, minima, maxima and the range per reef site and season (ESM Table S2).

Seasonal calcification rates of reef-building corals

We measured seasonal calcification rates of the three dominant coral genera between September 2012 and September 2013. *Porites* spp. fragments (massive growing *P. lobata* and *P. lutea* morphotypes) were included as representatives of the massive coral genus *Porites*, three acroporid morphotypes (*A. squarrosa, A. plantaginea, A. hemprichii*) were sampled to represent the branching coral genus *Acropora*, and fragments of the branching coral morphotype *Pocillopora verrucosa* were collected to represent the genus *Pocillopora* (in nearshore reef sites, this genus was not sufficiently present to assess calcification). In the following, we pool species into *Porites*, *Acropora*, and *Pocillopora* groups.

Coral fragments of similar size (5–10 cm) were collected from distinct colonies growing at least 5 m apart using hammer and chisel for massive corals or a dive knife for branching corals. Six to ten fragments were selected (avoiding fragments infested by endo- and epilithic organisms via visual inspection) and attached to a PVC frame using fishing line; each coral fragment was mounted between two bars of the frame, leaving a distance of ~25 cm to the bottom and top PVC bar (Fig. 2b). Fragments were acclimated in situ for 1–2 weeks before calcification measurements were started. Within this period, the tissue and skeleton of coral fragments overgrew the fishing line with no apparent tissue damage or health impact. Only visually healthy fragments at the beginning and end of the measuring periods were considered. Therefore, replicate numbers were reduced in some cases after the three-month period of deployment (see final replicate numbers in Fig. 1 and ESM Table S3).

Buoyant weight of fragments (Davies 1989) was measured at the beginning and end of each season: spring (10–13 and 24 March 2013 and 15–17 June 2013); summer (15–17 June 2013 and 9–11 September 2013); fall (16–18 and 25–26 September 2012 and 8–11 December 2012); and winter (8–11 December 2012 and 10–13 and 24 March 2013). Coral fragments were weighed in situ using a stainless-steel spring scale (Pesola, Switzerland, division 1 g, precision ±0.3 %), and weight increases over seasons

were determined. Over the course of seasonal measurements, missing or otherwise impacted coral colony fragments were replaced for the following season with newly collected fragments. Seasonal rates (G_{Coral}) were expressed as percent accretion of carbonate per day (Eq. 1, adopted from Ferrier-Pagès et al. 2000) using buoyant weight (Bw) increments over the calcification interval (season), normalized to the pre-season buoyant weight (Bw1) for each coral fragment, and divided by the days of the calcification interval (t).

$$G_{\mathrm{Coral}}\left(\%\,\mathrm{day}^{-1}\right) = \frac{\left[\left(\frac{\mathrm{Bw2}-\mathrm{Bw1}}{\mathrm{Bw1}}\right) \times 100\right]}{t} \quad (1)$$

Seasonal calcification rates of calcareous crusts (CC)

Calcification rates for CC were measured on seasonally sampled disposable microscope plastic slides (2.5 cm × 6 cm, Thermo Scientific Nunc Microscope Slides, USA) between December 2012 and December 2013. Deployment and sampling were conducted at the beginning and end of each season: spring (11–13 March 2013 to 15–18 June 2013); summer (15–18 June 2013 to 11–12 September 2013); fall (11–12 September 2013 to 9–11 December 2013); and winter (8–11 December 2012 to 11–13 March 2013).

Plastic/polyvinyl chloride (PVC) surfaces are commonly employed substrates for the measurement of carbonate accretion (Bak 1976; Kuffner et al. 2013). We used small slides due to their light weight, which allowed higher resolution and increased accuracy of the carbonate accretion measurements over relatively short periods of time (3 months). Prior to deployment, the clear and smooth slides were sandpapered resulting in a whitish, frosted surface. Six slides were deployed on an aluminum frame at every site (Fig. 2b). Some slides were lost during the deployment (see replicate numbers in Fig. 1 and ESM Table S3). Visual inspection of the recovered plastic slides indicated that CC was composed of green algae, brown algae, and coralline crusts. In a few cases, bryozoans were present, but neither coral recruits nor any other calcifying invertebrates were visually apparent. Upon recovery, slides were bleached for 12–14 h to remove organic material and dried for 48 h at 40 °C in an incubator (BINDER, Tuttlingen, Germany), and the dry mass (Dw1) comprising slide weight and carbonate accretion on both sides was obtained gravimetrically (Mettler Toledo XS205, $d = 0.01/0.1$ mg). Subsequently, slides were acidified in a 1:8 dilution of synthetic vinegar for 12–24 h to remove the entire carbonate crust and dried again (48 h at 40 °C), and weights of slides without carbonate (Dw2) were measured. Seasonally measured calcification rates were expressed as G_{CC} (mg cm^{-2} d^{-1}) by subtracting Dw2 from Dw1 and normalizing carbonate accretion to the slide surface area (cm^2) and the number of deployment days (t) following Eq. 2.

$$G_{\mathrm{CC}}\left(\mathrm{mg\,cm^{-2}\,day^{-1}}\right) = \frac{(\mathrm{Dw1}-\mathrm{Dw2})}{\mathrm{cm}^2 \times t} \quad (2)$$

Statistical analyses

Nonparametric multifactorial PERMANOVAs were employed to test for differences in coral seasonal calcification rates. Where calcification rates were repeatedly measured on one coral fragment across the seasons, tests for autocorrelation were performed to account for non-independence (Ljung and Box 1978; not significant for all repeated measurements). Next, coral calcification rates were square-root transformed and data from all corals were subjected to a multifactorial PERMANOVA (based on Euclidean distances and 999 permutations). Additionally, tests were run for each coral genus separately. Post-hoc pairwise tests were conducted for each significant factor independently. Further, we characterized the seasonal pattern in coral calcification rates; the increase in spring was quantified by calculating differences (as percentage increase) between the mean calcification rates in spring and the mean rates of the other seasons for each site.

CC data were tested in a similar way to coral data using the same transformation, PERMANOVA design, and specifications. Additionally, we characterized the seasonal pattern in CC calcification rates; the significant decrease in spring and summer was quantified by calculating differences (as percentage decrease) between mean calcification rates in spring and summer and mean rates in fall/winter.

Linear regressions were applied in each calcifier group to explore the relationships between calcification rates and the calcifiers' percent cover at the reef sites. Additionally, linear regressions were performed between the calcification rates of CC and the percent cover of the coral genera and between the percent cover of CC and percent cover of corals. Multifactorial analyses were conducted using the software package PRIMER-E v6 (PERMANOVA+). Statistica (StatSoft Inc. 2011, version 10) and SigmaPlot (Systat Software, version 11.0) were used for autocorrelation tests and linear regression.

Global comparison of calcification rates

For a comparative presentation of the calcification rates from our study, we compiled calcification data from coral reef regions around the globe (see ESM Appendix 1 for comparison of calcification data obtained with different measures). The most common metric reported in other studies is carbonate accretion normalized to surface area.

In order to compare CC calcification, we compared highest and lowest seasonal G_{CC} (mg cm^{-2} d^{-1}) values (ESM Table S3). For corals, calcification rates, G_{Coral} (mg cm^{-2} d^{-1}), were generated for a subset of samples, which represented all reef sites and were measured over two adjacent seasons (i.e., fall and winter; spring and summer; *Porites*, $n = 13$; *Acropora*, $n = 22$; *Pocillopora*, $n = 23$). Buoyant weight (Bw) increments over the two seasons were converted to dry weight increments (Dw) following Eq. 3 (Davies 1989):

$$\mathrm{Dw\,(mg)} = \frac{\mathrm{Bw\,(mg)}}{1 - \frac{\rho_{\mathrm{Seawater}}}{\rho_{\mathrm{Coral}}}} \quad (3)$$

We determined the surface area (cm^2) by wax dipping (Veal et al. 2010) and calculated overall calcification rates as dry weight increment per surface and day (mg cm^{-2} d^{-1}). Coral skeletal density values (ρ_{Coral}) of these coral fragments were determined according to Davies (1989) (Eq. 4), resulting in the mean densities of 2.72 ± 0.10, 2.87 ± 0.21, and 2.77 ± 0.14 g cm^{-3} (±SD) for *Porites*, *Acropora*, and *Pocillopora*, respectively. Further, for each reef at each sampling time, seawater density values ($\rho_{Seawater}$) were taken from the CTDs moored at the exposed sites (monthly means $\rho_{Seawater}$ ranged between 1.023 and 1.026 g cm^{-3}).

$$\rho_{\mathrm{Coral}}\left(\mathrm{g\,cm^{-3}}\right) = \frac{\rho_{\mathrm{Seawater}}}{1 - \left(\frac{\mathrm{Bw}}{\mathrm{Dw}}\right)} \quad (4)$$

Results

In this study, we assessed spatio-seasonal patterns of calcification of primary and secondary reef builders in the central Red Sea. The chosen study sites represent open sea exposed and sheltered lagoonal environments (see locations in Fig. 1; visual representation of habitats in Fig. 2a). We characterized the cross-shelf gradient by benthic cover assessment (Fig. 3) and measurements of water temperatures during the seasons (Fig. 4).

Benthic reef composition

Benthic transect data revealed differences between locations along the cross-shelf gradient (Fig. 3a; ESM Table S1); all sheltered sites were dominated by sandy bottom, rubble, and rock surface and characterized by a low percentage of live substrate (benthic organisms) (<40 %). Exposed sites in offshore and midshore reefs had the highest percentage of live benthos (>68 %) and the highest abundance (>48 %) of calcifying biota (hard coral and CC). The cover of calcareous crusts increased with distance from shore, from ~1 % in both nearshore sites and in the sheltered midshore site to 10 and 23 % in the midshore and offshore exposed sites, where coral cover was also greatest. In the offshore sheltered reef site, CC abundance was comparatively low (5 %).

Major scleractinian coral taxa belonging to the genera of *Acropora*, *Pocillopora*, *Porites* and constituted 32–56 % of the total hard coral cover in the study sites (Fig. 3b). Among the major taxa, the most widely abundant coral genus across the reefs was *Porites* (>~20 % of the total hard coral cover on most reefs). *Acropora* and *Pocillopora* were comparatively rare in nearshore reefs (both taxa present at 0.6–3 %), but prevalent in midshore exposed and offshore exposed and sheltered sites (13–27 %). Both genera increased in abundance with increasing distance from shore; while *Acropora* constituted 10 % in the midshore sheltered site, *Pocillopora* was only present at 3 %. In the midshore exposed site, both genera made up a larger percentage of the total coral cover (*Acropora*: 21 %, *Pocillopora*: 27 %).

Temperature profile

Data records from 7.5 to 9 m depth revealed increasing temperatures from spring onwards (mid-March), with maxima in summer (July and August), decreasing again during fall (late-September) and winter (December), and a minimum from January to early March (Fig. 4; ESM Table S2). The coldest season was winter (mid-December until mid-March) with a seasonal mean temperature of 26.4 ± 0.7 °C across sites (spanning a temperature range of 24.1–28.4 °C). The warmest season was summer (mid-June until mid-September) with a seasonal mean of 31.1 ± 0.7 °C across all sites (spanning a temperature range of 28.6–33.3 °C). The seasons representing rising and falling temperatures were spring (mid-March until mid-June; seasonal mean 28.0 ± 1.1 °C, range 26.2–30.8 °C) and fall (mid-September until mid-December; seasonal mean 30.0 ± 1.2 °C; range 27.0–32.2 °C). Standard deviations between 0.7 and 1.2 °C calculated per season pooled over the reef sites indicate smaller temperature differences between the sites, in comparison to the differences per site over the year (i.e., seasonal differences) that were characterized by higher standard deviations of 1.9–2.9 °C (ESM Table S2). The seasonal temperature differences between the lowest and highest temperature over the year recorded for each of the reef sites across the shelf were 6.6–9.0 °C.

Seasonal calcification of reef-building corals

Multifactorial PERMANOVAs were used to determine seasonal and spatial differences in calcification rates. The analysis of all seasonal coral rates revealed that coral 'genus' was the strongest source of variation (Pseudo-

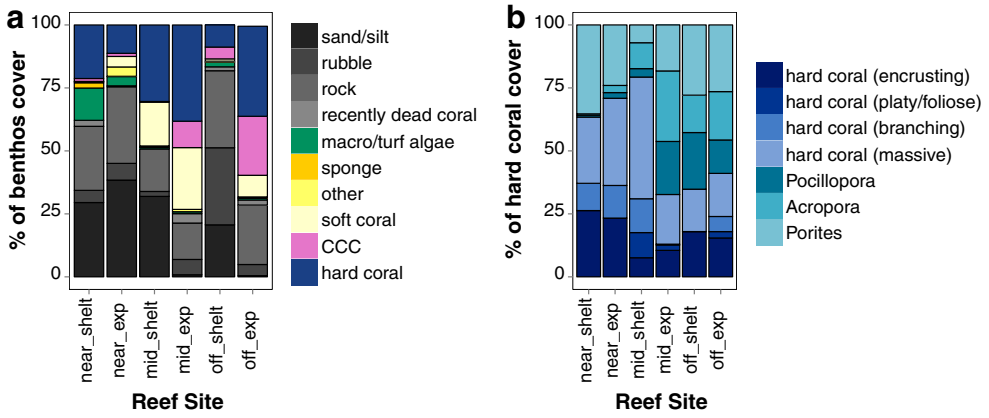

Fig. 3 Benthic composition at the six study sites depicted as means from six replicate rugosity transects per site. **a** Benthic categories as proportion of benthos cover (%). The category 'hard coral' sums all coral categories assessed. **b** The composition of hard coral cover is expressed as percent of total hard coral cover and includes the major reef-building coral taxa (*Porites* spp., *Acropora* spp., *Pocillopora* spp.) as well as other corals categorized to major morphological groups. CC, calcareous crusts; near, nearshore; mid, midshore; off, offshore; shelt, sheltered; exp, exposed

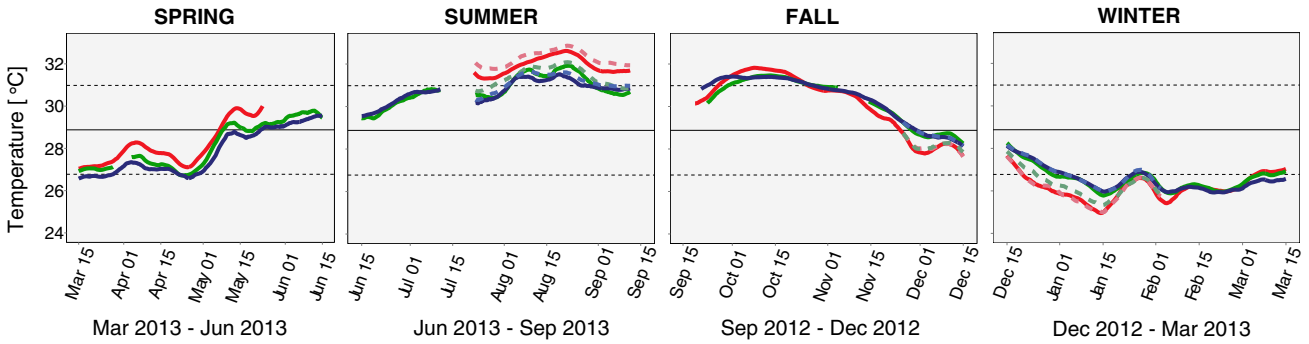

Fig. 4 Seasonal temperature profiles in the central Red Sea across study sites. Data are plotted for all study sites using a weekly moving average (*red* nearshore; *green* midshore; *blue* offshore; *continuous line* exposed; *dashed line* sheltered). All plots depict the annual mean temperature (*black line*) and the annual standard deviation (±SD: *black dashed lines*)

$F = 88.2$, $p_{(perm)} = 0.001$; Table 1, ESM Table S4). Further, a PERMANOVA on each coral genus separately revealed two patterns of coral calcification: calcification rates for *Porites* and *Acropora* significantly differed among seasons ($p_{(perm)} < 0.05$ for both genera; Table 1, ESM Table S4), but not among reefs or between exposures. *Pocillopora* calcification rates were different among seasons as well as between exposures (both factors $p_{(perm)} = 0.001$), but not among reefs. Common to all coral genera, highest calcification rates were observed during spring (Fig. 5, ESM Table S3). On average, spring calcification was 72 % higher in *Porites*, 74 % in *Acropora*, and

Table 1 PERMANOVA (fixed factors) results of seasonal calcification data

PERMANOVA design	$p_{(perm)}$ All corals	PERMANOVA design	$p_{(perm)}$ POR	$p_{(perm)}$ ACR	$p_{(perm)}$ POC	$p_{(perm)}$ CC
Coralgenus	**0.001**	–	–	–	–	–
Reef (coralgenus)	0.365	Reef	0.096	0.615	0.314	**0.001**
Exposure [reef (coralgenus)]	**0.001**	Exposure (reef)	0.06	0.094	**0.001**	**0.001**
Season {exposure [reef (coralgenus)]}	**0.001**	Season [exposure (reef)]	**0.017**	**0.033**	**0.001**	**0.001**

Significant results $p_{(perm)} < 0.05$ in bold

POR, *Porites*; ACR, *Acropora*; POC, *Pocillopora*; CC, calcareous crusts; $p_{(perm)}$, p value PERMANOVA

58 % higher in *Pocillopora* compared to the other seasons. There were only few cases when spring calcification was similar to, but still higher than, the other seasons (increase was <5 %, ESM Table S5). Of the three coral genera, only *Pocillopora* showed a significant difference in calcification rates between exposed and sheltered sites with rates higher at exposed sites (pairwise test results for midshore: $p_{(perm)} = 0.001$; offshore: $p_{(perm)} > 0.05$). Rates at most reefs were 8–55 % higher at the exposed sites than at sheltered sites, but the differences were largest at the exposed site of the midshore reef during winter and fall, with rates increased by up to 170 and 270 %, respectively. In addition, among all coral genera only calcification for *Pocillopora* had a significant linear relationship to percent cover of benthos ($R^2 = 0.40$, $p = 0.009$; Table 2, ESM Fig. S1a).

Seasonal calcification of calcareous crusts (CC)

Calcification patterns of CC (Fig. 5, ESM Table S3) differed from those of corals. Significant differences in CC calcification rates were found for the factors season, reef, and exposure (all: $p_{(perm)} = 0.001$; Table 1, ESM Table S6). Calcification rates of CC significantly increased with distance to shore and further increased at exposed sites compared to sheltered reef sites in the midshore and offshore reefs (both: pairwise test $p_{(perm)} = 0.001$). The highest seasonal mean calcification rate was measured at the exposed offshore site during winter (0.137 ± 0.025 mg cm^{-2} d^{-1}), while the lowest was at the sheltered nearshore site during summer (0.014 ± 0.002 mg cm^{-2} d^{-1}). Regarding the cross-shelf gradient, calcification at the offshore exposed site was 8.8-fold higher than at the nearshore sheltered site. Calcification rates were 50–123 % higher at the exposed reef sites (midshore and offshore reefs), but there was no significant difference between the exposed and sheltered site at the nearshore reef. Seasonality in CC was characterized by lower seasonal mean calcification rates during spring and summer at all sites (ESM Table S7). Spring and summer mean calcification rates were reduced by 13–66 % compared to the highest seasonal means in fall/winter for each respective site.

CC calcification rates and benthic cover were significantly linearly correlated ($R^2 = 0.82$ $p < 0.001$; Table 2, ESM Fig. S1b). Further, CC calcification was significantly correlated with the percent cover of the three coral taxa (*Porites*: $R^2 = 0.28$, $p = 0.01$; *Acropora*: $R^2 = 0.41$ $p = 0.001$; *Pocillopora*: $R^2 = 0.43$ $p < 0.001$, ESM Fig. S1c–e). Accordingly, CC percent cover correlated significantly with the coverage by coral taxa (*Porites*: $R^2 = 0.54$, $p < 0.001$; *Acropora*: $R^2 = 0.44$ $p < 0.001$; *Pocillopora*: $R^2 = 0.45$ $p < 0.001$; ESM Fig. S1f–h).

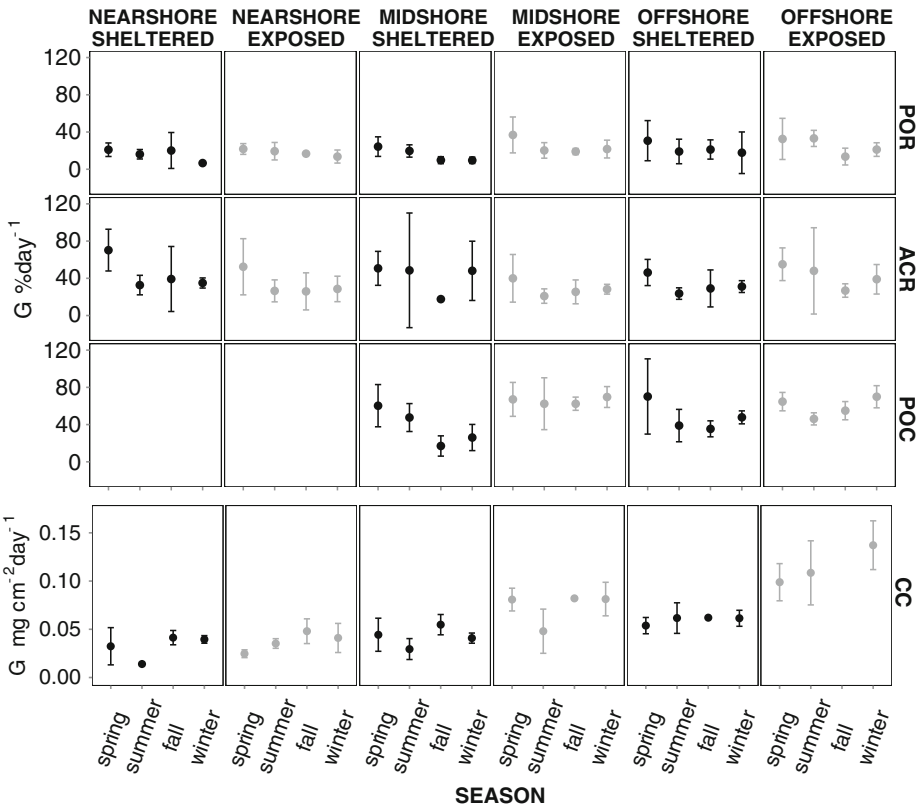

Fig. 5 Spatio-seasonal patterns of reef calcification for corals and calcareous crusts (CC). Plots are separated according to reef location (*columns*) with further subdivision for seasons on the *x*-axis. The *first three rows* show seasonal coral calcification rates as percent accretion per day [G_{Coral} (% d^{-1})] with *each row* showing one coral genus (POR, *Porites*; ACR, *Acropora*; POC, *Pocillopora*). Calcification for pocilloporid corals was not measured in nearshore reef sites. The *fourth row* shows CC calcification rates as dry weight accretion per surface area per day [G_{CC} (mg cm^{-2} d^{-1})]. *Filled circle*, means; *error bars*, standard deviation; color code: *gray*, exposed; *black*, sheltered

Table 2 Relationships between calcification rates and percent cover of calcifiers in the reef

Dependent variable	Explanatory variable	Linear regression	
		R^2	p
(a) Calcification rates vs. Percent cover of benthos			
POR	POR	0.07	0.221
ACR	ACR	0.03	0.452
POC	POC	**0.40**	**0.009**
(b) Calcification rates vs. Percent cover of benthos			
CC	CC	**0.82**	**<0.001**
CC	POR	**0.28**	**0.010**
CC	ACR	**0.41**	**0.001**
CC	POC	**0.43**	**<0.001**
(c) Percent cover of benthos vs. Percent cover of benthos			
CC	POR	**0.54**	**<0.001**
CC	ACR	**0.44**	**<0.001**
CC	POC	**0.45**	**<0.001**

(a) Linear regressions explore the relationships between calcification rates and percent cover of each calcifier. (b) Results of the linear regressions between calcification rates of CC and percent cover of each coral genus. (c) Results of the linear regressions between percent cover of CC and percent cover of the corals. (POR, *Porites*; ACR, *Acropora*; POC, *Pocillopora*; CC, calcareous crusts; significant results in bold)

Global comparison of calcification rates

Annual average calcification rates for *Porites* and *Pocillopora* from the central Red Sea were within the range of calcification rates from other regions (Table 3), while *Acropora* calcification rates were lower. In detail, *Porites* in the central Red Sea (1.46 ± 0.52 mg cm^{-2} d^{-1} ± SD) was intermediate in the range of values between 0.24 and 2.16 mg cm^{-2} d^{-1} from other regions (see below). *Pocillopora* calcified at an annual average rate of 0.92 ± 0.21 mg cm^{-2} d^{-1} in the central Red Sea and was at the higher end of the commonly measured range of 0.09–1.18 mg cm^{-2} d^{-1} reported from other studies. *Acropora* from the central Red Sea calcified at an average rate of 0.72 ± 0.17 mg cm^{-2} d^{-1} and was at the low end of the range reported by Goreau and Goreau (1959) for the Caribbean (0.84–3.06 mg cm^{-2} d^{-1}) and below the calcification reported from French Polynesia and Western Australia (around 1.0 mg cm^{-2} d^{-1}; Comeau et al. 2013; Foster et al. 2014). Calcification rates for *Acropora* and *Pocillopora* from aquaculture were far lower than field-based measurements (0.04–0.07 and 0.07–0.15 mg cm^{-2} d^{-1}, respectively). CC calcification rates from the central Red Sea (0.014–0.137 mg cm^{-2} d^{-1}) were in line with the rates measured elsewhere (lowest and highest reported values: 0.019 and 0.130 mg cm^{-2} d^{-1} both from the Caribbean); only Pari et al. (1998) reported a threefold higher maximum (0.310 mg cm^{-2} d^{-1}) measured in French Polynesia.

Discussion

Coral reef ecosystems critically rely on the reef carbonate framework produced by calcifying biota. In this study, we assessed spatial and seasonal reef calcification in corals and calcareous algae in the central Red Sea. We found that calcification in reef-building corals from the genus *Porites* and *Acropora* varied seasonally, while calcification in *Pocillopora* was influenced by season and site exposure. Importantly, calcification in secondary reef builders (CC) differed along the cross-shelf gradient and also with site exposure and season.

Spatial calcification and coral reef benthic composition

It has been rarely tested whether or how calcification rates play a role in structuring the benthic composition (Pratchett et al. 2015). In our study, we collected data on calcification rates and benthic reef abundance for selected coral genera to further understand how calcification performance relates to coral abundance in nearshore, midshore, and offshore reef sites. Among the corals in our study, only pocilloporid calcification rates were different among reef sites and were significantly related ($R^2 = 0.40$, $p < 0.01$) to their benthic abundances. *Pocillopora* is characterized as a 'weedy' and competitive taxon, often dominant in benthic assemblages (Darling et al. 2012). In our study, pocilloporids were less dominant and their calcification rates were also lower at sheltered than at exposed sites. This observation suggests that pocilloporid calcification rates may be a contributing factor to explain the taxon's dominance in exposed reef sites. In contrast, calcification rates of *Porites* and *Acropora* did not differ among sites but did correlate with their benthic abundance. In particular for *Acropora,* it is most evident that calcification rates, which were similar from nearshore to offshore reefs, cannot explain the increasing abundances from nearshore toward offshore reefs. Based on these data, we argue that benthic abundance of the corals studied here is less determined by their calcification performance than by other aspects such as limited coral settlement in nearshore locations. Lower settlement and recruitment rates may be a consequence of increased sedimentation or other coastal disturbances (Gilmour 1999), which are typical for nearshore reef sites (Cooper et al. 2007).

CC, aside from their role as secondary reef builders contributing to reef carbonate production and fortification

Table 3 Global comparison of annual calcification rates

Calcifier	Region	Calcification rate G (mg cm^{-2} d^{-1})	Study	Method
POR (*Porites* spp.)	Central Red Sea	1.46 (0.52)	This study	Buoyant weight
POR (*Porites furcata*)	Caribbean	0.24–2.16[b]	Goreau and Goreau (1959)	$Ca^{45}Cl_2$ incubations
POR (*Porites* sp.)	Japan	1.89	Comeau et al. (2014b)	Buoyant weight
POR (*Porites* sp.)	Hawaii	1.1	Comeau et al. (2014b)	Buoyant weight
POR (*Porites rus*)	French Polynesia	1.53 (0.07)	Comeau et al. (2013)	Buoyant weight
POR (*Porites* sp.)	French Polynesia	1.2	Comeau et al. (2014b)	Buoyant weight
ACR (*Acropora* spp).	Central Red Sea	0.72 (0.17)	This study	Buoyant weight
ACR (*Acropora eurystoma*)	Red Sea (Gulf of Aqaba)	0.96[c]	Schneider and Erez (2006)	TA depletion
ACR (*Acropora palmata*)	Caribbean	3.06[b]	Goreau and Goreau (1959)	$Ca^{45}Cl_2$ incubations
ACR (*Acropora cervicornis*)	Caribbean	0.84[b]	Goreau and Goreau (1959)	$Ca^{45}Cl_2$ incubations
ACR (*Acropora pulchra*)	Indian Ocean (Western Australia)	1.15	Foster et al. (2014)	Buoyant weight
ACR (*Acropora yongei*)	Indian Ocean (Western Australia)	1.31–2.02	Ross et al. (2015)	Buoyant weight
ACR (*Acropora pulchra*)	French Polynesia	1.41 (0.08)	Comeau et al. (2013)	Buoyant weight
ACR (*Acropora pulchra*)	French Polynesia	1.02 (0.05)[a]	Comeau et al. (2014a)	Buoyant weight
ACR (*Acropora millepora*)	Aquaculture	0.04–0.07	Schoepf et al. (2013)	Buoyant weight
POC (*Pocillopora* spp.)	Central Red Sea	0.92 (0.19)	This study	Buoyant weight
POC (*Pocillopora verrucosa*)	Red Sea	0.09–0.97[d]	Sawall et al. (2015)	TA depletion
POC (*Pocillopora damicornis*)	Indian Ocean (Western Australia)	0.66	Foster et al. (2014)	Buoyant weight
POC (*Pocillopora damicornis*)	Indian Ocean (Western Australia)	0.34–0.90	Ross et al. (2015)	Buoyant weight
POC (*Pocillopora damicornis*)	Japan	1.18	Comeau et al. (2014b)	Buoyant weight
POC (*Pocillopora damicornis*)	Hawaii	0.75	Comeau et al. (2014b)	Buoyant weight
POC (*Pocillopora damicornis*)	Hawaii	0.17–0.38[e]	Clausen and Roth (1975)	$Ca^{45}Cl_2$ incubations
POC (*Pocillopora damicornis*)	French Polynesia	0.69 (0.08)	Comeau et al. (2013)	Buoyant weight
POC (*Pocillopora damicornis*)	French Polynesia	0.6	Comeau et al. (2014b)	Buoyant weight
POC (*Pocillopora damicornis*)	Aquaculture	0.07–0.15	Schoepf et al. (2013)	Buoyant weight
CC	Central Red Sea	0.014–0.137	This study	Dry weight
CC	Caribbean	0.036	Bak (1976)	Dry weight
CC	Caribbean	0.130	Kuffner et al. (2013)	Dry weight
CC	Caribbean	0.019–0.035[f]	Mallela and Perry (2007)	Dry weight
CC	Caribbean	0.029 (0.019)[f]	Mallela (2013)	Dry weight
CC	French Polynesia	0.05–0.310	Pari et al. (1998)	Dry weight

Locations from the central Red Sea (this study), the Indo-Pacific, and the Caribbean are considered.

POR *Porites*, ACR *Acropora*, POC *Pocillopora*, CC calcareous crusts

Values are reported as a regional range, as an average value as mean (SD), or if labeled [a] as an average value mean (SE). Values were converted to mg cm^{-2} d^{-1} from: [b] μg Ca cm^{-2} h^{-1}, [c] μmol $CaCO_3$ cm^{-2} h^{-1}, [d] μmol $CaCO_3$ cm^{-2} d^{-1}, [e] ng $CaCO_3$ mm^{-2} h^{-1}, [f] g m^{-2} yr^{-1}

of the reef framework (Mallela 2007; Perry and Hepburn 2008), fulfill another crucial ecological role by providing settlement cues and substrate for the larvae of reef-building corals (Heyward and Negri 1999). Our data support this argument by showing a significant positive relationship of CC calcification rates and percent cover with the abundances of the three important reef builders *Porites*, *Acropora*, and *Pocillopora*. Since studies focusing on CC are scarce (Mallela 2013), our conclusions emphasize the importance of incorporating the assessment of CC calcification and community dynamics in future coral reef studies and monitoring efforts.

Seasonal calcification and temperature dependency

Among various physicochemical factors that can influence calcification in corals and CC (e.g., aragonite saturation state, nutrient, and light availability; Chalker 1981; Gattuso et al. 1998; Chisholm 2000; Ferrier-Pagès et al. 2000), temperature has been demonstrated to be a dominant driver (Borowitzka

and Larkum 1987; Martin and Gattuso 2009; Cooper et al. 2012; Castillo et al. 2014). In this study, calcification in corals and CC from the central Red Sea was significantly driven by season. Further, temperature differences on the seasonal scale were larger than differences among sites across the shelf (i.e., nearshore, midshore, and offshore). Consequently, we consider seasonal temperature differences an essential component of the seasonal variation in calcification rates. In the Gulf of Aqaba (northern Red Sea region), temperatures and community net calcification were found to be positively correlated at a temperature range of 23–27 °C, but not for temperatures above 27 °C (Silverman et al. 2007). Our long-term measurements of seasonal calcification rates do not allow deduction of exact temperature optima for these calcifiers. But importantly, our data indicate that the optimal conditions for calcification may be similar in the three coral genera (*Porites*, *Acropora,* and *Pocillopora*) and lie within the temperature range of spring (min–max 26.2–30.8 °C). Further, for CC we can show that both spring and summer (min–max 26.2–33.3 °C) are associated with reduced seasonal calcification rates, which implies that temperatures in this range may be detrimental to CC calcification.

Calcification maxima are observed when local seawater temperatures meet the temperature optimum of the local calcifiers. Typically calcification maxima have been reported for the warmest season of the year (summer), for example for *Siderastrea siderea* from the northern Caribbean (Kuffner et al. 2013), *Acropora formosa* from Western Australia (Crossland 1984), CC from Japan (Hibino and van Woesik 2000), and net community calcification in Hawaii (Atkinson and Grigg 1984). Importantly, in the northern Red Sea, calcification maxima were reported for summer (Silverman et al. 2007; Sawall et al. 2015), whereas in the southern region highest calcification rates were measured in *P. verrucosa* during winter, the coldest season of the year (Sawall et al. 2015), indicating that calcification peaks are determined by optimal prevailing temperature profiles. Here, we demonstrate that in the central Red Sea calcification maxima of three coral genera (*Porites*, *Acropora*, and *Pocillopora*) were not observed during the warmest season of the year (summer), but during spring. This is in accordance with the recently reported north to south calcification patterns observed for *P. verrucosa* in the Red Sea where Sawall et al. (2015) found that calcification maxima occurred during summer in the north and during winter in the south. Our results can be interpreted as an indication that summer temperatures in the central Red Sea exceed the optimum local calcification temperature of three coral species and CC. A similar observation was recently reported from Western Australia (Foster et al. 2014), where the absence of a summer peak in calcification has been interpreted as a consequence of anomalously high summer temperatures in that region.

Calcification in corals versus calcareous crusts (CC)

Our measurement of calcification rates revealed different trends for corals and CC. We show that coral calcification rates vary mainly with season. By contrast, CC calcification rates are strongly influenced by cross-shelf position, site exposure, and seasonality. This may be attributable to physiological differences between corals (Tambutté et al. 2011) and CC (Borowitzka and Larkum 1987) and also shows that environmental parameters other than temperature are important. Putatively, increased turbidity and decreased irradiance in nearshore reef locations (Cooper et al. 2007) might explain the highly reduced nearshore calcification rates of CC, which rely solely on photosynthesis (Chisholm 2000; Edinger et al. 2000; Fabricius and De'ath 2001). Coral calcification, by comparison, seemed to be less affected by the higher turbidity and lower irradiance in nearshore sites. Taken together, our results show that CC calcification is much more variable over distance to shore and seasons in comparison to coral calcification. This suggests that CC calcification is more sensitive to spatio-temporal differences in environmental conditions and may thus be more susceptible to environmental change. Considering the importance of CC in shaping the reef structure, their sensitivity to changing environmental conditions may have substantial consequences for coral reef benthic communities.

Global comparison of calcification rates from the central Red Sea

Although calcification studies are numerous and cover many locations globally, our effort toward a global comparison of calcification rates indicated that it remains difficult to make accurate comparisons, due to inconsistencies in methodologies or the normalization of measurements (see ESM Appendix 1). Our comparative evaluation based on annual average calcification rates from studies using a similar approach to ours demonstrates that the range of calcification in two major coral genera (*Porites* and *Pocillopora*) and CC were very similar between the Red Sea and the Caribbean or Indo-Pacific (Table 3). For the coral *Acropora*, we show that calcification rates in our study were at the lower end of the global range, although Red Sea conditions, i.e., high light penetration and high carbonate saturation state, are anticipated to be beneficial for calcification. We conclude that Red Sea coral reef calcifiers are neither more nor less productive in terms of carbonate accretion, despite these favorable conditions. Indications that summer temperatures exceed the optima of reef calcifiers in this region (this study; Sawall et al. 2015) in conjunction with increasing temperatures as a result of environmental change (Raitsos et al. 2011) pose

detrimental effects to calcifiers, which may be counterbalancing the presumably beneficial effects of the Red Sea environment for calcification. The future persistence of coral reefs depends, besides other factors, on the rate of calcification in reef-building biota. Therefore, monitoring and evaluation of calcification rates in the Red Sea are crucial for the assessment of ecosystem stability. We hope that our study provides a baseline of calcification rates in primary and secondary reef builders for this region and serves as a foundation for comparative efforts to quantify impact of future environmental change.

Acknowledgments We thank the team from the Coastal and Marine Resources Lab (CMOR) at King Abdullah University of Science and Technology (KAUST) for logistics and operations at sea (E. Al-Jahdali, A. Al-Jahdali, G. Al-Jahdali, R. Al-Jahdali, H. Al-Jahdali, F. Mallon, D. Pallett) and for the assistance with the deployment of oceanographic instruments (CTD) (L. Smith, S. Mahmoud). We would like to acknowledge additional field assistance by M. Ziegler, P. Müller, R. van der Merwe, M. Ochsenkühn, A. O'Rourke, and S. Baumgarten. Research reported in this publication was supported by KAUST.

Open Access This article is distributed under the terms of the Creative Commons Attribution 4.0 International License (http://creativecommons.org/licenses/by/4.0/), which permits unrestricted use, distribution, and reproduction in any medium, provided you give appropriate credit to the original author(s) and the source, provide a link to the Creative Commons license, and indicate if changes were made.

References

Abu-Ghararah ZH (1997) Assessment of land-based sources and activities affecting the marine environment in the Red Sea and Gulf of Aden. UNEP Regional Seas Reports and Studies No 166

Atkinson MJ, Grigg RW (1984) Model of a coral reef ecosystem. II. Gross and net benthic primary production at French Frigate Shoals, Hawaii. Coral Reefs 3:13–22

Bak RPM (1976) The growth of coral colonies and the importance of crustose coralline algae and burrowing sponges in relation with carbonate accumulation. Neth J Sea Res 10:285–337

Borowitzka MA, Larkum AWD (1987) Calcification in algae: mechanisms and the role of metabolism. Crit Rev Plant Sci 6:1–45

Cantin NE, Cohen AL, Karnauskas KB, Tarrant AM, McCorkle DC (2010) Ocean warming slows coral growth in the central Red Sea. Science 329:322–325

Carricart-Ganivet JP (2004) Sea surface temperature and the growth of the West Atlantic reef-building coral *Montastraea annularis*. J Exp Mar Bio Ecol 302:249–260

Carricart-Ganivet JP, Cabanillas-Terán N, Cruz-Ortega I, Blanchon P (2012) Sensitivity of calcification to thermal stress varies among genera of massive reef-building corals. PLoS One 7:e32859

Castillo KD, Ries JB, Bruno JF, Westfield IT (2014) The reef-building coral *Siderastrea siderea* exhibits parabolic responses to ocean acidification and warming. Proc R Soc Lond B Biol Sci 281:20141856

Chalker BE (1981) Simulating light-saturation curves for photosynthesis and calcification by reef-building corals. Mar Biol 63:135–141

Chisholm JRM (2000) Calcification by crustose coralline algae on the northern Great Barrier Reef, Australia. Limnol Oceanogr 45:1476–1484

Clausen CD, Roth AA (1975) Estimation of coral growth-rates from laboratory 45Ca-incorporation rates. Mar Biol 33:85–91

Comeau S, Carpenter RC, Edmunds PJ (2014a) Effects of irradiance on the response of the coral *Acropora pulchra* and the calcifying alga *Hydrolithon reinboldii* to temperature elevation and ocean acidification. J Exp Mar Bio Ecol 453:28–35

Comeau S, Edmunds PJ, Spindel NB, Carpenter RC (2013) The responses of eight coral reef calcifiers to increasing partial pressure of CO_2 do not exhibit a tipping point. Limnol Oceanogr 58:388–398

Comeau S, Carpenter RC, Nojiri Y, Putnam HM, Sakai K, Edmunds PJ (2014b) Pacific-wide contrast highlights resistance of reef calcifiers to ocean acidification. Proc R Soc Lond B Biol Sci 281:20141339

Cooper TF, O'Leary RA, Lough JM (2012) Growth of Western Australian corals in the Anthropocene. Science 335:593–596

Cooper TF, Uthicke S, Humphrey C, Fabricius KE (2007) Gradients in water column nutrients, sediment parameters, irradiance and coral reef development in the Whitsunday region, central Great Barrier Reef. Estuar Coast Shelf Sci 74:458–470

Cooper TF, De'ath G, Fabricius KE, Lough JM (2008) Declining coral calcification in massive *Porites* in two nearshore regions of the northern Great Barrier Reef. Glob Chang Biol 14:529–538

Crossland CJ (1984) Seasonal variations in the rates of calcification and productivity in the coral *Acropora formosa* on a high-latitude reef. Mar Ecol Prog Ser 15:135–140

Darling ES, Alvarez-Filip L, Oliver TA, McClanahan TR, Côté IM (2012) Evaluating life-history strategies of reef corals from species traits. Ecol Lett 15:1378–1386

Davies PS (1989) Short-term growth measurements of corals using an accurate buoyant weighing technique. Mar Biol 101:389–395

Davis KA, Lentz SJ, Pineda J, Farrar JT, Starczak VR, Churchill JH (2011) Observations of the thermal environment on Red Sea platform reefs: a heat budget analysis. Coral Reefs 30:25–36

Edinger EN, Limmon GV, Jompa J, Widjatmoko W, Heikoop JM, Risk MJ (2000) Normal coral growth rates on dying reefs: are coral growth rates good indicators of reef health? Mar Pollut Bull 40:404–425

Fabricius K, De'ath G (2001) Environmental factors associated with the spatial distribution of crustose coralline algae on the Great Barrier Reef. Coral Reefs 19:303–309

Ferrier-Pagès C, Gattuso JP, Dallot S, Jaubert J (2000) Effect of nutrient enrichment on growth and photosynthesis of the zooxanthellate coral *Stylophora pistillata*. Coral Reefs 19:103–113

Foster T, Short JA, Falter JL, Ross C, McCulloch MT (2014) Reduced calcification in Western Australian corals during anomalously high summer water temperatures. J Exp Mar Bio Ecol 461:133–143

Gattuso J-P, Frankignoulle M, Bourge I, Romaine S, Buddemeier RW (1998) Effect of calcium carbonate saturation of seawater on coral calcification. Glob Planet Change 18:37–46

Gilmour J (1999) Experimental investigation into the effects of suspended sediment on fertilisation, larval survival and settlement in a scleractinian coral. Mar Biol 135:451–462

Goatley CHR, Bellwood DR (2011) The roles of dimensionality, canopies and complexity in ecosystem monitoring. PLoS One 6:e27307

Goreau TF (1963) Calcium carbonate deposition by coralline algae and corals in relation to their roles as reef-builders. Ann N Y Acad Sci 109:127–167

Goreau TF, Goreau NI (1959) The physiology of skeleton formation in corals. II. Calcium deposition by hermatypic corals under various conditions in the reef. Biol Bull 117:239–250

Graham NAJ (2014) Habitat complexity: coral structural loss leads to fisheries declines. Curr Biol 24:R359–R361

Heyward AJ, Negri AP (1999) Natural inducers for coral larval metamorphosis. Coral Reefs 18:273–279

Hibino K, van Woesik R (2000) Spatial differences and seasonal changes of net carbonate accumulation on some coral reefs of the Ryukyu Islands, Japan. J Exp Mar Bio Ecol 252:1–14

Houlbrèque F, Ferrier-Pagès C (2009) Heterotrophy in tropical scleractinian corals. Biol Rev 84:1–17

Kleypas JA, McManus JW, Menez LAB (1999) Environmental limits to coral reef development: where do we draw the line? Am Zool 39:146–159

Kuffner IB, Hickey TD, Morrison JM (2013) Calcification rates of the massive coral *Siderastrea siderea* and crustose coralline algae along the Florida Keys (USA) outer-reef tract. Coral Reefs 32:987–997

Ljung GM, Box GEP (1978) On a measure of lack of fit in time series models. Biometrika 65:297–303

Lough JM, Barnes DJ (2000) Environmental controls on growth of the massive coral *Porites*. J Exp Mar Bio Ecol 245:225–243

Mallela J (2007) Coral reef encruster communities and carbonate production in cryptic and exposed coral reef habitats along a gradient of terrestrial disturbance. Coral Reefs 26:775–785

Mallela J (2013) Calcification by reef-building sclerobionts. PLoS One 8:e60010

Mallela J, Perry C (2007) Calcium carbonate budgets for two coral reefs affected by different terrestrial runoff regimes, Rio Bueno, Jamaica. Coral Reefs 26:129–145

Marshall AT, Clode P (2004) Calcification rate and the effect of temperature in a zooxanthellate and an azooxanthellate scleractinian reef coral. Coral Reefs 23:218–224

Martin S, Gattuso J-P (2009) Response of Mediterranean coralline algae to ocean acidification and elevated temperature. Glob Chang Biol 15:2089–2100

Muscatine L (1990) The role of symbiotic algae in carbon and energy flux in reef corals. In: Dubinsky Z (ed) Coral reefs, Ecosystems of the world, vol 25. Elsevier, Amsterdam, pp 75–87

Pari N, Peyrot-Clausade M, Le Champion-Alsumard T, Hutchings P, Chazottes V, Gobulic S, Le Champion J, Fontaine MF (1998) Bioerosion of experimental substrates on high islands and on atoll lagoons (French Polynesia) after two years of exposure. Mar Ecol Prog Ser 166:119–130

Perry CT, Hepburn LJ (2008) Syn-depositional alteration of coral reef framework through bioerosion, encrustation and cementation: taphonomic signatures of reef accretion and reef depositional events. Earth Sci Rev 86:106–144

Perry C, Edinger E, Kench P, Murphy G, Smithers S, Steneck R, Mumby P (2012) Estimating rates of biologically driven coral reef framework production and erosion: a new census-based carbonate budget methodology and applications to the reefs of Bonaire. Coral Reefs 31:853–868

Pratchett MS, Anderson KD, Hoogenboom MO, Widman E, Baird AH, Pandolfi JM, Edmunds PJ, Lough JM (2015) Spatial, temporal and taxonomic variation in coral growth—implications for the structure and function of coral reef ecosystems. Oceanogr Mar Biol Annu Rev 53:215–295

Raitsos DE, Hoteit I, Prihartato PK, Chronis T, Triantafyllou G, Abualnaja Y (2011) Abrupt warming of the Red Sea. Geophys Res Lett 38:L14601

Ross CL, Falter JL, Schoepf V, McCulloch MT (2015) Perennial growth of hermatypic corals at Rottnest Island, Western Australia (32°S). PeerJ 3:e781

Sawall Y, Al-Sofyani A, Hohn S, Banguera-Hinestroza E, Voolstra CR, Wahl M (2015) Extensive phenotypic plasticity of a Red Sea coral over a strong latitudinal temperature gradient suggests limited acclimatization potential to warming. Sci Rep 5:8940

Schneider K, Erez J (2006) The effect of carbonate chemistry on calcification and photosynthesis in the hermatypic coral *Acropora eurystoma*. Limnol Oceanogr 51:1284–1293

Schoepf V, Grottoli AG, Warner ME, Cai W-J, Melman TF, Hoadley KD, Pettay DT, Hu X, Li Q, Xu H, Wang Y, Matsui Y, Baumann JH (2013) Coral energy reserves and calcification in a high-CO_2 world at two temperatures. PLoS One 8:e75049

Silverman J, Lazar B, Erez J (2007) Effect of aragonite saturation, temperature, and nutrients on the community calcification rate of a coral reef. J Geophys Res 112:C05004

Steiner Z, Erez J, Shemesh A, Yam R, Katz A, Lazar B (2014) Basin-scale estimates of pelagic and coral reef calcification in the Red Sea and Western Indian Ocean. Proc Natl Acad Sci U S A 111:16303–16308

Tambutté S, Holcomb M, Ferrier-Pagès C, Reynaud S, Tambutté É, Zoccola D, Allemand D (2011) Coral biomineralization: from the gene to the environment. J Exp Mar Biol Eco 408:58–78

Veal CJ, Carmi M, Fine M, Hoegh-Guldberg O (2010) Increasing the accuracy of surface area estimation using single wax dipping of coral fragments. Coral Reefs 29:893–897

Wilkinson C (2008) Status of coral reefs of the world: 2008. Global Coral Reef Monitoring Network and Reef and Rainforest Research Centre, Townsville, Australia

Wooldridge SA (2014) Assessing coral health and resilience in a warming ocean: why looks can be deceptive. Bioessays 36:201400074